Journal of the National Academy OF Forensic Engineers®

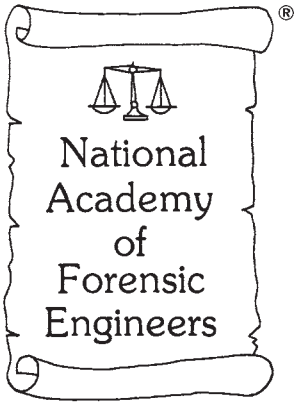

Vol. 32 No. 1 June 2015

Generalized Deformation and Total Velocity Change Analysis with Missing Vehicle Stiffness Coefficients; G-DaTA ΔV™

By Jerry S. Ogden, P.E. (NAFE 561F)

Abstract

Analysis of vehicle deformation from impacts largely relies upon A and B stiffness coefficients for vehicle structures in order to approximate the velocity change and accelerations produced by an impact. While frontal impact stiffness factors for passenger vehicles, light trucks, vans, and sport utility vehicles are relatively prevalent for modern vehicles, stiffness factors for rear and side structures — as well as heavy vehicles, buses, recreational vehicles, trailers, motorcycles, and even objects — are essentially non-existent.

This paper presents methods developed from the principles of energy, momentum, restitution, tire forces, and rotational mechanics applicable to deformation profile analysis by eliminating the need for structural A and B stiffness coefficients for both vehicles involved in a two-vehicle collision. This is often achievable for most collision combinations. Additionally, the application of these developed principles to RICSAC (Research Input for Computer Simulation of Automobile Collisions) test data will demonstrate the accuracy achieved by using this methodology — even when the structural stiffness values for both vehicles are available, but only the frontal stiffness values of one vehicle are utilized.

Keywords

Forensic engineering, force deflection, damage analysis, missing vehicle stiffness, velocity change from damage, motorcycle, heavy vehicles, object impacts, G-DaTA ΔV™

Background

One of the earliest approaches to analyze vehicle damage was developed through the work done by Campbell in the early 1970s[1]. Campbell observed a linear relationship between fixed barrier impact speeds and residual deformation of a vehicle structure during full-scale impact testing using General Motors vehicles.

Further research into this matter was conducted by McHenry and others at Cornell Aeronautical Lab (currently known as CALSPAN) through the development of SMAC (Simulation Model for Automobile Collisions), which improved upon Campbell's earlier observations. Specifically, McHenry noted that vehicles behave like linear energy-dissipating springs. The studies by Campbell and McHenry were later adapted into a computer analysis package known as the Collision Reconstruction of Accident Speeds on Highways Program, or CRASH, which was a first approximation tool for use in estimates necessary for the SMAC analysis. The current edition of this program is known as CRASH III, with other clone or similar variants in use today[2].

Current common practices for motor vehicle damage analysis, such as standardizing measurement protocols[3,4] and a widespread use of modernized equations that account for rotational effects[5], have developed into accurate, reliable, and commonly used means for determining collision severity levels and collision velocities. This is assuming proper structural stiffness values for each colliding vehicle characteristic (for both vehicles and the specific impacted surface) are available. Although extensive test data is presently available from vehicle manufacturers and test laboratories for the determination of frontal stiffness coefficients (for many passenger vehicles and light trucks), few tests are available for such determination as they relate to side and rear surface vehicle specific stiffness coefficients. Additionally, there is limited data available for heavy vehicle frontal barrier impacts (including semi-tractors

Jerry S. Ogden, M.S., P.E., P.O. Box 621519, Littleton, Colorado 80162-1519; (303) 795-1515; jogden@OEC4N6.com

and buses), for frontal stiffness coefficient determination. Accordingly, either additional expensive and time-consuming barrier tests are needed to fill these gaps, or another method of analysis is needed.

In general, the limiting assumptions and limitations of CRASH III and similar CRASH-based programs are as follows:

- Deformation energy is equal to the impact kinetic energy loss.
- Collisions are inelastic, and the centroids of damage reach a common velocity.
- Sliding between vehicles occurs during the separation phase of the impact and not during the approach velocity change phase; therefore, it is not accounted for in the velocity change analysis.
- Tire-ground forces are negligible (non-conservative forces external to the impact) or very small as compared to the collision force and do not need to be accounted for.
- Damage profile measurements are limited by evenly spaced measurements of 2, 4, 6 or more deformation depths over uniform spaced measurement widths.
- Vehicle structural stiffness is defined by categories of vehicles by type (i.e., car, truck, van), and wheelbase lengths, all assumed to have similar inertial and stiffness characteristics.

This paper presents the equations derived from engineering principles that allow for the following analysis considerations not currently considered by CRASH-type analysis procedures:

- Develop analysis methodologies that eliminate the dependence upon multiple structural stiffness coefficients for permanent vehicle structural deformation analysis, regardless of the impacted surface and vehicle type involved.
- Develop analysis methodologies that account for oblique and offset collisions that result in principal directions of force that do not pass through the mass centers of vehicles and produce rotation.
- Develop analysis methodologies that account for friction due to the colliding surfaces of vehicles sliding during the approach velocity change of an impact.
- Develop analysis methodologies that account for forces external to the impact produced by tire-ground forces during the approach velocity change of an impact.
- Establish important relationships regarding impact forces as they relate to motor vehicle collisions and vehicle deformation properties.

Basic Equations

The basic CRASH algorithms are derived from sound principles and applications of Newton's laws of motion, Hooke's law, and the conservation of energy and momentum. For central, single degree of freedom impacts — where the vehicle-to-vehicle colliding system is treated as a simple harmonic oscillating spring system — the basic force-deflection equation is as follows:

$$F = (A + B \cdot c^R) \cdot w \quad (1)$$

Where, A = (force / length), which is the force per unit depth to initiate damage to the vehicle and applied throughout the application of external forces resulting from the collision

B = (force / area), the generalized spring constant associated with resistance to continued deformation/spring compression of the vehicle structure as a result of the external forces of the collision

c^R = (length), residual inward deformation measured post-collision, perpendicular to the damaged surface

w = (length), width of deformation profile between measured points

Equation 1 is a basic expression that relates to a uniform deformation profile of uniform deformation depth across its entire width. For more complex damage profiles, the impact force is approximated using what will be defined as the *Central Impact Force-Deflection Model*:

$$\sum_{j=0}^{n} F_j^I = \sum_{j=0}^{n} \left(A_i + B_i \cdot \Delta c_j^R \right) \cdot \Delta w_j \quad (2)$$

Where, $\Delta c_j^R = \frac{\left(c_j^R + c_{j+1}^R \right)}{2}$ = (length) average deformation depth between measured points j and j+1, j=0…n measurements across differential width

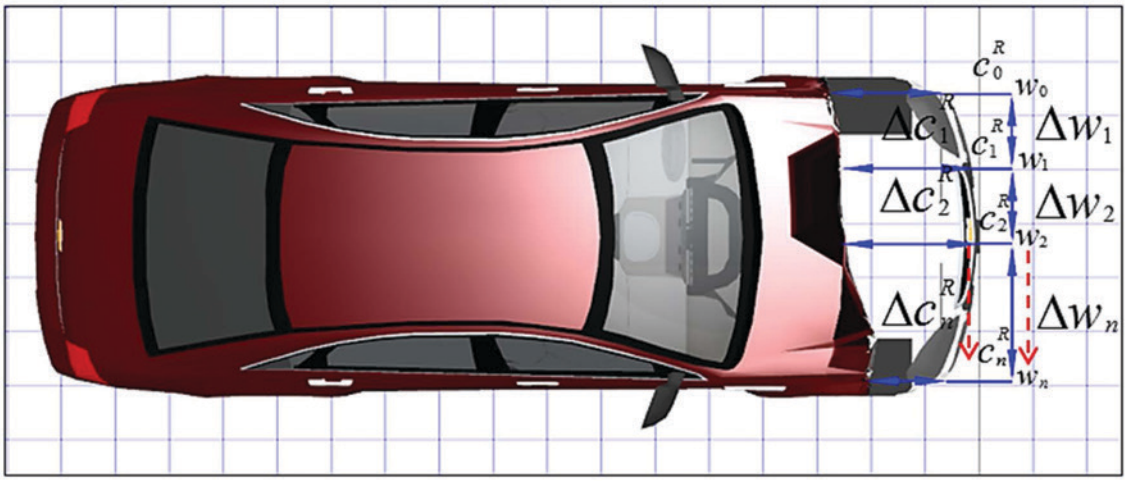

Description of point measured	Distance from Left Front (0)	Distance to undamaged profile
Left front corner	w0: +0 cm (0 inches)	c0: +81 cm (32 inches)
Left front frame rail	w1: +46 cm (18 inches)	c1: +81 cm (32 inches)
Center bumper reinforcement bar	w2: +92 cm (36 inches)	c2: +71 cm (28 inches)
C3…C(n-1)	w3…w(n-1)	c3…c(n-1)
Right front corner	w(n): +183 cm (72 inches)	c(n): +51 cm (20 inches)

So that, $\Delta c_1^R = \frac{c_0^R + c_1^R}{2} = \frac{(81cm + 81cm)}{2} = 81cm$ (32 inches)

$\Delta c_2^R = \frac{c_1^R + c_2^R}{2} = \frac{(81cm + 71cm)}{2} = 76cm$ (30 inches), and so forth.

And, $\Delta w_1 = w_1 - 0_0 = (46cm - 0cm) = 46cm$ (18 inches)

$\Delta w_2 = w_2 - w_1 = (92cm - 46cm) = 46cm$ (18 inches), and so forth.

Figure 1
Measured damage dimensions.

$\Delta w_j = \left(w_{j+1} - w_j\right)$ = (length) width of deformation interval between measured points j and j+1, j=0…n measurements across differential width

Figure 1 shows an example of how the deformation depth and width measurements are made and tabulated for ease of use.

Integrating Equation 2 with respect to the deformation depth, Δc^R, provides the work done over the deformation profile due to the collision impulse. This integral operation produces what is hereto defined as the *Central Impact Work/Energy Model* of Equation 3.

$$\sum_{j=0}^{n} F_j^I = \sum_{j=0}^{n} \left(A_i + B_i \cdot \Delta c_j^R\right) \cdot \Delta w_j$$

$$E_i = \sum_{j=0}^{n} \int_0^{\Delta w_j} F_j^I \cdot d\Delta w_j = \sum_{j=0}^{n} \int_0^{\Delta c_j^R} \left(\left(A_i + B_i \cdot \Delta c_j^R\right) \cdot \Delta w_j\right) \cdot d\Delta c_j^R$$

$$E_i^{damage} = \sum_{j=0}^{n} \left(A_i \cdot \Delta c_j^R + \frac{B_i \cdot \left(\Delta c_j^R\right)^2}{2} + \frac{A_i^2}{2 \cdot B_i} \right) \cdot \Delta w_j \quad (3)$$

Where, A_i and B_i = unique structural stiffness values for the impacted surface of the i[th] vehicle (for a two-vehicle system, i = 1..2)

Δc_j^R = the residual deformation, or "crush", of the i[th] deformation measured on the i[th] vehicle

perpendicular to the damaged surface from its undamaged dimensions

Δw_j = width of the j[th] deformation, measured parallel to the damaged surface of the i[th] vehicle

By utilizing a numerical method of determining the work, E_i, done by the impact force, F_i, for each vehicle, i = 1..2, the restriction imposed by CRASH-type programs of 2, 4, or 6 evenly spaced deformation measurements is eliminated. Utilizing Equations 2 and 3 allows for the analysis of deformation with as many measurements as needed and at any measured width in order to accurately describe a vehicle's damage profile.

The basic equations for a completely plastic central impact that does not consider restitution, tire-ground forces, rotation, or inter-vehicle friction are the basis of the earlier CRASH-based computer programs, and the basic velocity change magnitude equations are as follows:

$$\Delta V1 = \sqrt{\frac{2 \cdot m_2 \cdot \left(E1_{damage} + E2_{damage}\right)}{m_1 \cdot \left(m_1 + m_2\right)}} \quad (4)$$

$$\Delta V2 = \sqrt{\frac{2 \cdot m_1 \cdot \left(E1_{damage} + E2_{damage}\right)}{m_2 \cdot \left(m_1 + m_2\right)}} \quad (5)$$

Central Impacts Accounting for Restitution and Tire-Ground Forces

This author has previously published methods for utilizing vehicle deformation profiles for determining velocity changes of collinear, central impacts that account for the effects of restitution and tire-ground forces of an impact[6,7]. Restitution effects are greatest at lower impact velocity change levels ($0 < \Delta v \leq 10$ mph) and will range between $0.2 \leq e \leq 0.6$ for most collisions with the highest restitution values occurring at the lowest velocity change levels of the range, and will approach $e \approx 0$ at higher impact velocity change levels ($\Delta v > 20$ mph).

Tire forces may contribute significantly to the external impulses acting upon a low velocity change impact ($\Delta v \leq 10$ mph), but are often considered insignificant for higher level impacts. Examples of when tire forces may not be negligible are as follows:

- Collinear rear-end collision event where front vehicle (target vehicle) is braking when struck by rear vehicle (bullet vehicle).
- Broadside impact where side-struck vehicle (target vehicle) slides broadside against the roadway surface during the impact.
- Impact with a heavy vehicle either broadside or while brakes are applied on the heavy vehicle and/or trailer.
- Any collision configuration where a motion constraint, such as wheel blocking, curb, wall or barrier, etc., may be present at impact.

Figure 2 shows how the external impulse of braking force interacts external to the forces of an impact event. It is important to note that the impulse of tire-ground forces is external to the collision impulse in that tire-ground forces are "non-conservative" impulse constraint forces acting upon the system during the approach velocity change, which is common for many constrained holonomic and non-holonomic dynamic systems[8].

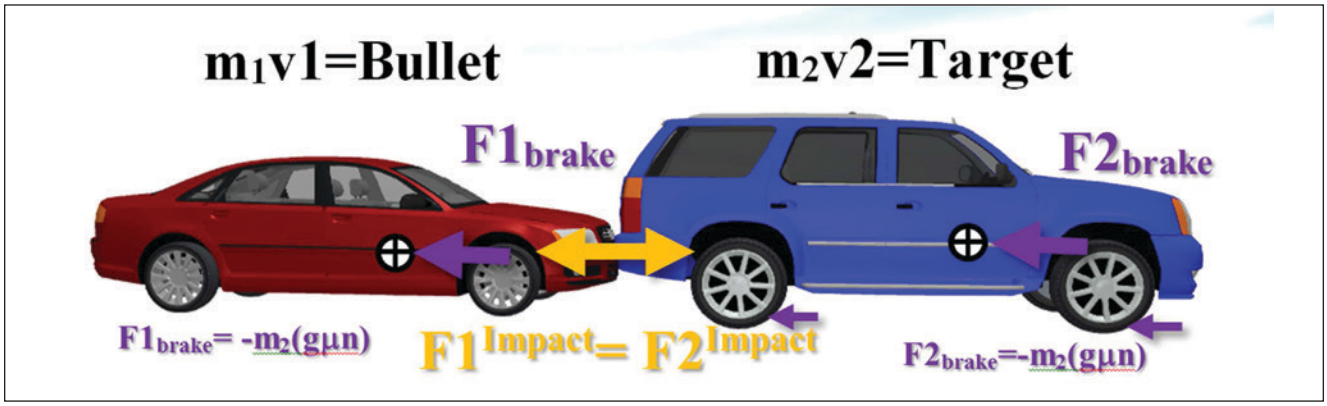

Figure 2
Tire-ground forces external to collision impulse (front vehicle braking).

The basic equations derived while accounting for restitution effects during the approach velocity change as well as non-conservative external tire-ground impulse constraint forces are hereto defined as the *Central Impact Force-Deflection Velocity Change Equations:*

Tire-ground contribution vehicle 1:

$$F1^{brake} = m_1 \cdot a1^{brake} = m_2 \cdot (g\mu n)$$

$$m_1 \cdot \frac{\Delta v1^{brake}}{\Delta t} = m_2 \cdot (g\mu n)$$

$$\Delta v1^{brake} = \frac{m_2 \cdot (g\mu n) \cdot \Delta t}{m_1}$$

Tire-ground contribution vehicle 2:

$$F2^{brake} = m_2 \cdot a2^{brake} = -m_2 \cdot (g\mu n)$$

$$m_2 \cdot \frac{\Delta v2^{brake}}{\Delta t} = -m_2 \cdot (g\mu n)$$

$$\Delta v2^{brake} = \frac{-m_2 \cdot (g\mu n) \cdot \Delta t}{m_2} = -(g\mu n) \cdot \Delta t$$

$$\Delta V1 = (1+e)\sqrt{\frac{2 \cdot m_2 \cdot \left(E1^{damage} + E2^{damage}\right)}{m_1 \cdot (m_1 + m_2)}} + \frac{m_2 \cdot (g \cdot \mu \cdot n) \cdot \Delta t}{m_1} \quad (6)$$

$$\Delta V2 = (1+e)\sqrt{\frac{2 \cdot m_1 \cdot \left(E1^{damage} + E2^{damage}\right)}{m_2 \cdot (m_1 + m_2)}} - (g \cdot \mu \cdot n) \cdot \Delta t \quad (7)$$

The previous equations (as derived) are limited to central impacts or collinear impacts that produce negligible rotation to either vehicle due to impact offset. It is important to again stress that these velocity change magnitudes are vectors along a single coordinate line of action, so that the absolute value of the velocity change for the bullet vehicle *(ΔV1)* is *increased* by tire-ground impulse constraint forces, while the absolute value of the velocity change for the target vehicle *(ΔV2)* is *decreased* by tire-ground impulse constraint forces.

Oblique and Offset Impacts

Oblique and offset impacts result from applied forces that do not act through the mass centers of at least one of the colliding vehicles. As such, the applied force creates a pure force couple, resulting in rotation or at least the potential for rotation to one or both colliding vehicles along with translation, or at least the potential for translational motion. When rotation occurs, tire forces are often counteracting to the moment created by the oblique force application. **Figure 3** shows the effects of an oblique impact upon the overall planar motion (x, y, ϕ) of a vehicle, resulting in rotation about the z-axis in yaw (ϕ).

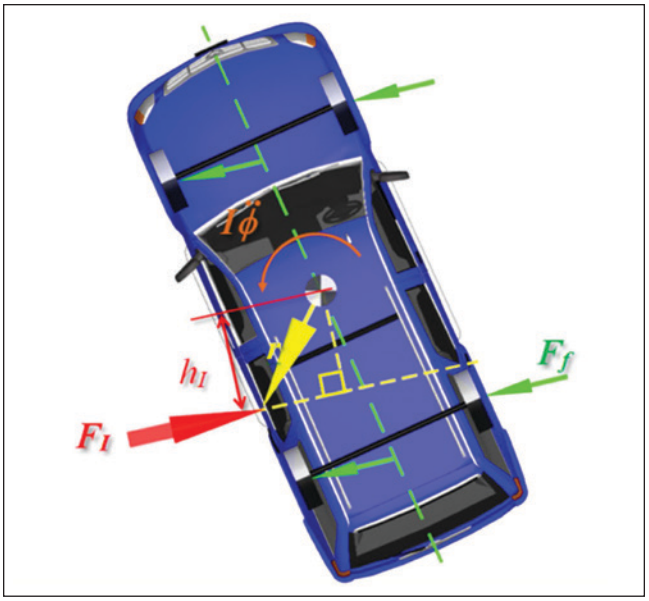

Figure 3
Moment arm applied to produce rotation about mass center.

The mass moment of inertia is an object's measure of resisting rotational acceleration, just as mass is the measure of a body's resistance to translational acceleration. The moment of inertia of an object is a function of shape and mass. If the moment of inertia is determined about a primary axis that passes through the mass center of an object, it is called a *polar moment of inertia*[9]. Using polar moments of inertia, hereto simply referred to as *mass moment of inertia*, and determining dynamics about polar (or primary) axes makes analysis much easier, and is routinely used for motor vehicle collision analysis with few exceptions. The moment of inertia about any axis, to include those that do not pass through the mass center of a body, can be determined using the parallel axis theorem if the polar moment of inertia is known. Likewise, the polar moment of inertia of a composite or oddly shaped object can be determined using the parallel axis theorem with respect to each of the individual moments of inertia of the geometric shapes that make up the total body shape. In

general, the moment of inertia is determined as the sum of the product of all the differential mass elements of the body, *dm*, and the square of its distance from the axis of rotation, *r*.

$$dI = r^2 \cdot dm$$
$$I = \sum_{i=1}^{n} r_i^2 \cdot m_i \quad (8)$$

Another method of describing the polar moment of inertia of an object with great utility is known as the *radius of gyration, k_g, which* assumes all the mass, *m*, is concentrated within an equivalent radius about a primary axis that passes through the mass center of the object[9,10].

$$I = m \cdot k_g^2 \quad (9)$$

Because passenger vehicles, light trucks, and vans are non-homogeneous complex geometric shapes, the mass moment of inertia is determined experimentally using tilt table measurements, or more commonly from best-fit equations derived from experimental data. Garrott presented data from the NHTSA Light Vehicle Inertial Parameter Data Base containing measured vehicle inertial parameters of 356 tested vehicles, plus tilt table data for 168 vehicles[11] as a follow-up to an initial paper presenting an algorithm for determining moments of inertia for the curb weight of unloaded vehicles by distinct vehicle classifications[12]. Neptune presented a method for determining the yaw moment of inertia (I_{zz}, or mass moment of inertia about the *z-axis* of the vehicle) based upon the method presented by Garrott, but allowing for the addition of occupant and cargo weights[13], providing greater utility for collision analysis. Equation 10 from the Neptune paper reduces to the best fit algorithm developed by Garrott when the vehicle is unloaded.

$$I_{zz} = \frac{m_{curb}}{K_G} \cdot \left(L^2 + b^2\right) \cdot \left(K_M \cdot \left(\frac{m_{loaded} - m_{curb}}{m_{loaded}}\right)\right) \quad (10)$$

Where, I_{zz} = yaw moment of inertia (about *z-axis*)
m_{curb} = curb mass of vehicle (unloaded)
m_{loaded} = loaded mass of vehicle (curb plus occupants and cargo)
L = total length of vehicle
b = maximum width of vehicle
K_G = geometric empirically determined constant (see **Figure 4**)
K_M = geometric empirically determined constant (see **Figure 4**)

Vehicle type	K_G	K_M	R^2
All combined	13.1	0.696	0.85
Passenger car	13.8	0.769	0.86
Light truck	13.4	0.750	0.92
SUV	12.2	0.656	0.76
Light van	12.3	0.642	0.90

Figure 4
Yaw moment of inertia empirical constants.

Consider the vehicle in **Figure 5**. The principal direction of force, PDOF, acting upon the centroid of the damaged frontal surface is angled from the residual deformation measurements, c_n^R, which are recorded parallel to the primary longitudinal axis, using the

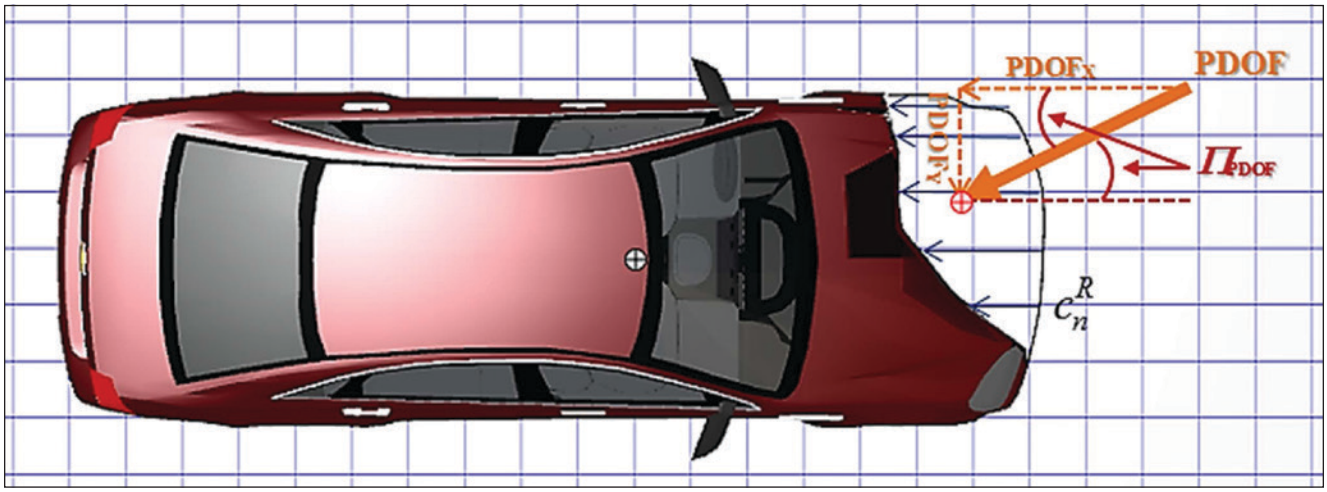

Figure 5
Oblique impact PDOF acting at damage centroid.

undamaged surface (in this case, front bumper) as the datum line to measure from for a frontal deformation profile. Therefore, using Equation 2 to determine the impact force only accounts for the longitudinal component of the force without accounting for the fact that the total collision force acts along the angle of the PDOF, $\prod^{PDOF}$. Such an assumption may lead to a significant under-approximation of the total force acting upon the vehicle structure for an oblique impact.

Therefore, the total force of the impact, $\mathbf{F}_{\text{PDOF}}$, must be determined. The following derivation for $\mathbf{F}_{\text{PDOF}}$ from Equation 2 results in the *Generalized Impact Force-Deflection Model*.

$$Fx = F^{PDOF} \cdot \cos(\Pi^{PDOF})$$

$$F^{PDOF} = Fx \cdot \frac{1}{\cos(\Pi^{PDOF})}$$

$$F^{Gen} = \sum_{j=0}^{n} \left(A_i + B_i \cdot \Delta c_j^R\right) \cdot \frac{\Delta w_j}{\cos(\Pi_i^{PDOF})} \tag{11}$$

Where, A_i, B_i, Δc_j^r, Δw_j are as previously defined
$\prod_i^{\text{PDOF}}$ = angle of the PDOF acting upon the i^{th} vehicle

The *Generalized Impact Force-Deflection Model* of Equation 11 provides the magnitude of the total external force acting upon the damage centroid of a vehicle during an oblique or offset impact. This is equal in magnitude but opposite in direction of application to the external force applied through the damage centroid for the opposing vehicle in accordance with Newton's third law. Equation 11 is a more complete and generalized statement of the *Central Impact Force-Deflection Model* stated by Equation 2, in that as $\prod_{PDOF}$ approaches 0 for Equation 11, then $\boldsymbol{F}^{Gen} \rightarrow \sum_{j=0}^{n} F_j^I$ of Equation 2. As a generalized equation, Equation 11 has broader application to a multitude of varying impact configurations that include central, collinear, offset, and oblique impacts.

The *Generalized Force-Deflection Model* provides the means by which the total force acting upon a vehicle during an impact is determined, regardless of whether the impact is a central or oblique collision event. Similar methods previously used in formulating the expression for the work necessary to deform the vehicle spring system (resulting from a central impact) are utilized when determining the work necessary to produce permanent deformation to the i^{th} vehicle (where i=1..2 for a two vehicle system) involved in an oblique or central impact event, when the deformation depth and width measurements for each vehicle are known or knowable. This results in the *Oblique Impact Work/Energy Model* represented by Equation 12.

$$\sum_{j=0}^{n} \int_{0}^{\Delta c_j^{total}} \left(F_{pdof}\right) \cdot d\Delta c_j^{total} = \sum_{j=0}^{n} \left(\int_{0}^{\Delta c_j^{total}} \left(\left(A_i + B_i \cdot \Delta c_j^R\right) \cdot \frac{\Delta w_j}{\cos(\Pi_{PDOF})} \right) \cdot d\Delta c_j^{total} \right)$$

$$\Delta c_j^{total} = \frac{\Delta c_j^R}{\cos(\Pi_{PDOF})} \qquad \text{Integrate then substitute value for total deformation}$$

$$\sum_{j=0}^{n} \int_{0}^{\Delta c_j^{total}} \left(F_{pdof}\right) \cdot d\Delta c_j^{total} = \sum_{j=0}^{n} \left(A_i \cdot \Delta c_j^R + \frac{B_i \cdot \left(\Delta c_j^R\right)^2}{2} + \frac{A_i^2}{2 \cdot B_i} \right) \cdot \frac{\Delta w_j}{\cos(\Pi_{PDOF})^2} \tag{12}$$

Work due to friction often results from oblique impacts where the corner or narrow "contact" region on a striking vehicle slides along the relative extended length of the "surface" on a struck vehicle so that the overall *contact*

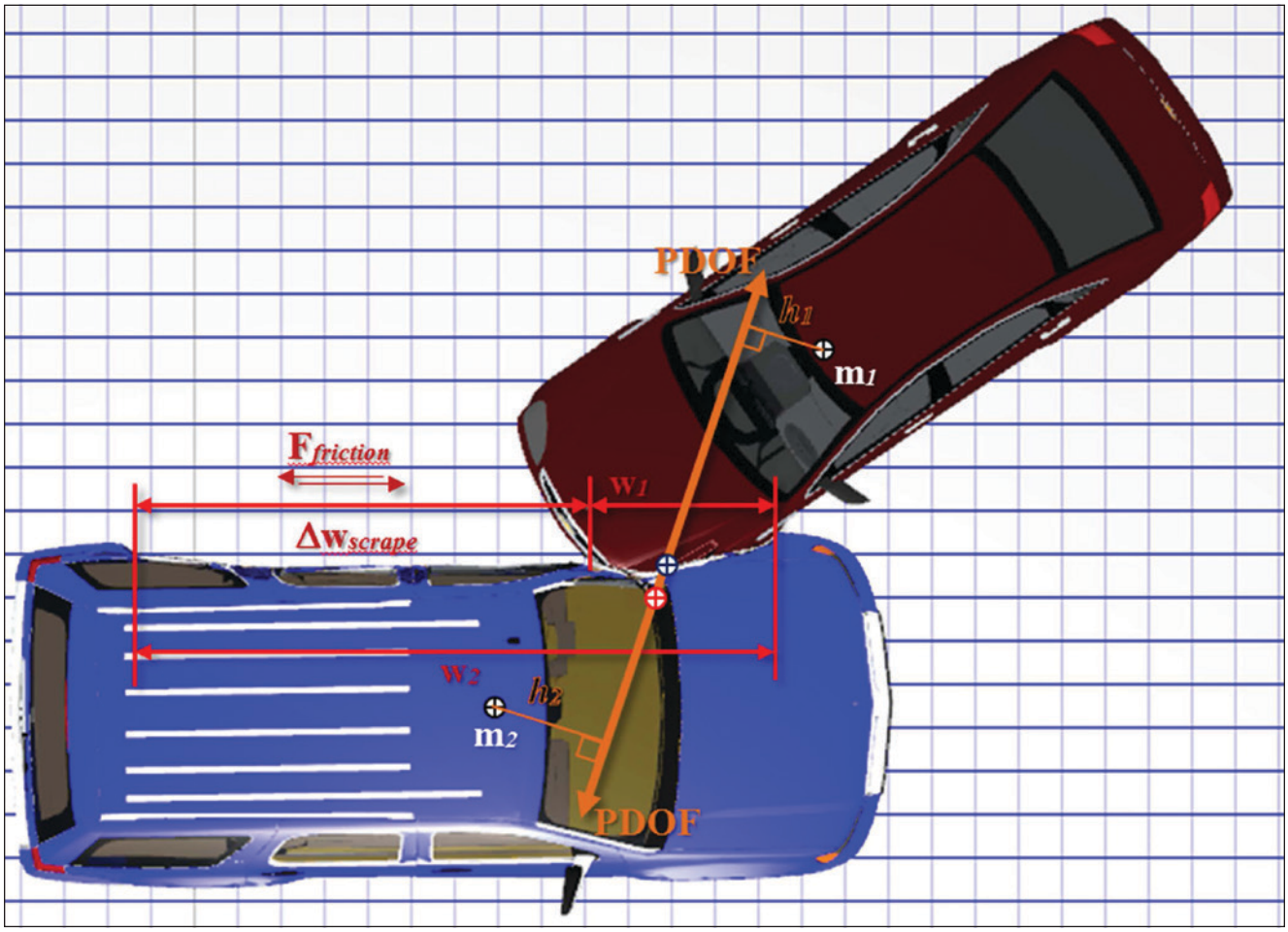

Figure 6
Friction of extended contact, scraping impacts.

and *surface* damage regions between the vehicles are dissimilar. The resultant *approach phase* force (due to impact determined in Equation 11) does not change as a result of the inter-vehicular friction between the two surfaces, since the frictional forces between the vehicles act at (or near) perpendicular to the applied impact force at maximum impulse, thus not contributing to the impulsive force of the impact. Therefore, inter-vehicular friction results in an extended tail of the impulse curve due to an extended contact time period between the vehicles during approach and separation. **Figure 6** demonstrates how to determine the net contact distance due to inter-vehicle friction.

Consider the contact between the two vehicles shown in **Figure 6**. The width of contact on the striking vehicle, m_1, is concentrated on the left front corner, while the width of contact on the struck vehicle, m_2, extends across a much broader width of contact, which is due to scraping between the vehicles during separation. The width of scraping may be difficult to directly measure on each vehicle, but is easily and accurately approximated by the difference in contact widths.

$$\Delta w_{scrape} = w_2 - w_1 \tag{13}$$

The work done within the region of scraping is dissipated energy due to kinetic friction as the two surfaces slide against each other, as well as continued deformation resulting from an extended impact force impulse — until final separation occurs. Even though the inter-vehicular friction occurs during the separation phase of the impact, the additional inward deformation from separation should be considered as part of the deformation profile when calculating the total force and total work in Equations 11 and 12. The basic equation for kinetic friction between any two surfaces is as follows:

$$F^{friction} = \mu_k \cdot F^{Normal} \tag{14}$$

Where, μ_k = coefficient of kinetic friction

F^{Normal} = normal force acting between two sliding surfaces

Because the force due to friction is acting between the two sliding vehicle surfaces while in contact, the friction force acting upon m_1 must be equal in magnitude but opposite in application to the friction force acting upon m_2.

$$\begin{aligned} m_1 \cdot a_1 \cdot \mu_k &= m_2 \cdot a_2 \cdot \mu_k \\ m_1 \cdot g \cdot n_1 \cdot \mu_k &= m_2 \cdot g \cdot n_2 \cdot \mu_k \\ m_1 \cdot g \cdot \left(\frac{m_2}{m_1+m_2}\right) \cdot \mu_k &= m_2 \cdot g \cdot \left(\frac{m_1}{m_1+m_2}\right) \cdot \mu_k \end{aligned} \tag{15}$$

$$F_2^{friction} = m_2 \cdot g \cdot \left(\frac{m_1}{m_1+m_2}\right) \cdot \mu_k \tag{16}$$

The work done due to friction is the integral of the force over the work distance, Δw_{scrape}, which results in the additional work due to friction that must be accounted for during the approach phase of the collision.

$$\int_0^{w_1} F_1^{Friction} \cdot dw_1 = \int_0^{w_1} \left(m_1 \cdot g \cdot \mu_k \cdot \left(\frac{m_2}{m_1+m_2}\right)\right) \cdot d\Delta w_{scrape}$$

$$\int_0^{\Delta w_{scrape}} F_2^{Friction} \cdot dw_2 = \int_0^{\Delta w_{scrape}} \left(m_2 \cdot g \cdot \mu_k \cdot \left(\frac{m_1}{m_1+m_2}\right)\right) \cdot d\Delta w_{scrape}$$

$$E_1^{friction} = m_1 \cdot g \cdot \mu_k \cdot \left(\frac{m_2}{m_1+m_2}\right) \cdot \Delta w_{scrape} \tag{17}$$

$$E_2^{friction} = m_2 \cdot g \cdot \mu_k \cdot \left(\frac{m_1}{m_1+m_2}\right) \cdot \Delta w_{scrape} \tag{18}$$

Studies have reported the coefficient of kinetic friction for vehicle-to-vehicle contact ranges between $0.3 \leq \mu_k \leq 1.1$, depending upon the angle of impact[14,15]. The highest friction levels were associated with impacts nearing parallel approach angles at contact (sideswipe), while the lower friction levels were associated with oblique impacts. By inspection of Equations 17 and 18, frictional effects may be a significant consideration for impacts that produce large discrepancies between the damage widths of the vehicles. Additionally, the longer the vehicles remain in contact during the approach velocity change phase, the longer the external tire/surface impulse affects the overall velocity change levels for both vehicles. Therefore, the consideration of work due to friction (if evidence of sliding is present) should provide a more accurate analysis of the collision event.

The development of the oblique impact and friction work equations allow for a more generalized analysis of work to cause deformation. A complete generalized model should account for the effects of an oblique collision upon the residual damage approximations across the damage width as well as the contributions of friction between sliding surfaces in contact during the approach phase of the impact. The total work done on the system is the sum of the work during the approach and departure velocity change phases, which are defined here as the *Generalized Impact Work/Energy Model* of Equations 19 and 20.

$$\begin{aligned} E_1^{Gen} &= E_1^{Oblique} + E_1^{friction} \\ &= \sum_{j=0}^{n} \left(A_1 \cdot \Delta c1_j^R + \frac{B_1 \cdot \left(\Delta c1_j^R\right)^2}{2} + \frac{A_1^2}{2 \cdot B_1} \right) \cdot \Delta wl_j \cdot \left(1 + \tan^2\left(\Pi_{PDOF1}\right)\right) + m_1 \cdot g \cdot \mu_k \cdot \left(\frac{m_2}{m_1+m_2}\right) \cdot \Delta w_{scrape} \end{aligned} \tag{19}$$

$$\begin{aligned} E_2^{Gen} &= E_2^{Oblique} + E_2^{friction} \\ &= \sum_{j=0}^{n} \left(A_2 \cdot \Delta c2_j^R + \frac{B_2 \cdot \left(\Delta c2_j^R\right)^2}{2} + \frac{A_2^2}{2 \cdot B_2} \right) \cdot \Delta w2_j \cdot \left(1 + \tan^2\left(\Pi_{PDOF2}\right)\right) + m_2 \cdot g \cdot \mu_k \cdot \left(\frac{m_1}{m_1+m_2}\right) \cdot \Delta w_{scrape} \end{aligned} \tag{20}$$

Figure 6 showed an oblique collision between two vehicles and the moment arms, h_1 and h_2, for the torque applied to vehicles 1 and 2, respectively. The torque applied to each vehicle is given by Equation 21, and Newton's second law states that the sum of the torques for a conservative system (which impact impulse is identified as a conservative contribution to the system) must be equal to zero. Equation 9 also provided an important relationship between the yaw moment of inertia of a vehicle about the primary vertical axis, I_{zz}, and the radius of gyration of the effective mass as it rotates around the primary vertical axis.

$$\tau = r \times F_i = h \cdot F^{magnitude} = I_{cm}\ddot{\phi} \qquad (21)$$

$$I_{zz} = m \cdot k^2$$

(restatement of Equation 9)

Where, $\boldsymbol{\tau}$ = torque

$\mathbf{r}$ = vector from point of rotation to applied force

$\mathbf{F_I}$ = applied force vector from collision

$F_{magnitude}$ = magnitude of applied force

I_{cm} = polar mass moment of inertia (about axis through mass center)

$\ddot{\phi}$ = rotational acceleration

h_1 = perpendicular moment arm for impact induced moment

k = radius of gyration about principle axis of rotation

m = mass of vehicle

Additionally, the acceleration at the damage centroid of each vehicle, or common velocity point, between the vehicles has the following relationships with respect to each vehicle:

Vehicle 1:

$$a1_{common} = a1_{cm} + h_1 \cdot \ddot{\phi}_1$$

$$\ddot{\phi}_1 = \frac{a1_{common} - a1_{cm}}{h_1}$$

Vehicle 2:

$$a2_{common} = a2_{cm} + h_2 \cdot \ddot{\phi}_2$$

$$\ddot{\phi}_2 = \frac{a_{common} - a2_{cm}}{h_2}$$

The rotational acceleration of each vehicle produced by the force couple can be related in the following manner.

Vehicle 1:

$$F^{Gen} \cdot h_1 = I1_{zz} \cdot \ddot{\phi}_1$$

$$h_1 \cdot m_1 \cdot a1_{cm} = m_1 \cdot k1_g^2 \cdot \left(\frac{a1_{common} - a1_{cm}}{h_1} \right)$$

Vehicle 2:

$$F^{Gen} \cdot h_2 = I2_{zz} \cdot \ddot{\phi}_2$$

$$h_2 \cdot m_2 \cdot a2_{cm} = m_2 \cdot k2_g^2 \cdot \left(\frac{a2_{common} - a2_{cm}}{h_2} \right)$$

Grouping like terms allows for the solution for the force at the center of mass with respect to the radius of gyration and moment arm of the force applied at the common point of contact between the vehicles.

Vehicle 1:

$$h_1^2 \cdot \left(m_1 \cdot a1_{cm} \right) = m_1 \cdot k1_g^2 \cdot \left(a1_{common} - a1_{cm} \right)$$

$$m_1 \cdot a1_{cm} \cdot \left(k1_g^2 + h_1^2 \right) = m_1 \cdot a1_{common} \cdot k1_g^2$$

$$m_1 \cdot a1_{cm} = \left(\frac{k1_g^2}{k1_g^2 + h_1^2} \right) \cdot m_1 \cdot a1_{common}$$

Vehicle 2:

$$h_2^2 \cdot \left(m_2 \cdot a2_{cm} \right) = m_2 \cdot k2_g^2 \cdot \left(a2_{common} - a2_{cm} \right)$$

$$m_2 \cdot a2_{cm} \cdot \left(k2_g^2 + h_2^2 \right) = m_2 \cdot a2_{common} \cdot k2_g^2$$

$$m_2 \cdot a2_{cm} = \left(\frac{k2_g^2}{k2_g^2 + h_2^2} \right) \cdot m_2 \cdot a2_{common}$$

Substitute Equation 9 for the radius of gyration for each vehicle:

Vehicle 1:

$$m_1 \cdot a1_{cm} = \left(\frac{\frac{I1_{zz}}{m_1}}{\frac{I1_{zz}}{m_1} + h_1^2} \right) \cdot m_1 \cdot a1_{common}$$

$$\text{Where, } \gamma_1 = \left(\frac{I1_{zz}}{I1_{zz} + m_1 \cdot h_1^2} \right)$$

$$F1_{cm} = (m_1 \cdot \gamma_1) \cdot \frac{\Delta v1_{common}}{\Delta t}$$

Vehicle 2:

$$m_2 \cdot a2_{cm} = \left(\frac{\frac{I2_{zz}}{m_2}}{\frac{I2_{zz}}{m_2} + h_2^2} \right) \cdot m_2 \cdot a2_{common}$$

$$\text{Where, } \gamma_2 = \left(\frac{I2_{zz}}{I2_{zz} + m_2 \cdot h_2^2} \right)$$

$$F2_{cm} = (m_2 \cdot \gamma_2) \cdot \frac{\Delta v2_{common}}{\Delta t}$$

Vehicle 1 total momentum change:

$$F1_{cm} \cdot \Delta t = \Delta p_1 = (m_1 \cdot \gamma_1) \cdot \Delta v1_{common}$$

Vehicle 2 total momentum change:

$$F2_{cm} \cdot \Delta t = \Delta p_2 = (m_2 \cdot \gamma_2) \cdot \Delta v2_{common}$$

The values of γ_1 and γ_2 are defined here as the *effective rotational (dynamic) mass ratio* for vehicle 1 and vehicle 2, respectively. The above final equation simply states that the total change in momentum for each vehicle is equivalent to the velocity change at the point of common contact between the vehicles times the *effective rotational mass ratio* produced by the oblique impact. The culmination of the consideration of restitution, tire forces, friction and rotational contributions to the collision leads to the *Generalized Impact Force-Deflection Velocity Change Model,* which determines the *total velocity change* magnitudes for each of the vehicles as follows:

$$\Delta V_1^{Gen} = (1+e)\sqrt{\frac{2 \cdot m_2 \cdot \gamma_2 \cdot \left(E_1^{Gen} + E_2^{Gen}\right)}{m_1 \cdot \gamma_1 \cdot (m_1 \cdot \gamma_1 + m_2 \cdot \gamma_2)}} + \frac{m_2 \cdot (g \cdot \mu \cdot n) \cdot \Delta t}{m_1} \quad (22)$$

$$\Delta V_2^{Gen} = (1+e)\sqrt{\frac{2 \cdot m_1 \cdot \gamma_1 \cdot \left(E_1^{Gen} + E_2^{Gen}\right)}{m_2 \cdot \gamma_2 \cdot (m_1 \cdot \gamma_1 + m_2 \cdot \gamma_2)}} - (g \cdot \mu \cdot n) \cdot \Delta t \quad (23)$$

Where, e = coefficient of restitution for collision level

γ_1 and γ_2 = effective rotational (dynamic) mass ratios

μ = roadway coefficient of friction

n = braking efficiency and/or brake force distribution as a decimal ($0 \le n \le 1.0$)

Δt = impulse time period during approach velocity change

E_1^{Gen} and E_2^{Gen} = the total work determined by Equations 19 and 20

Solving for the impulse time period when considering the impact force, rotational effects and all external forces acting upon the system results in Equation 24.

$$\Delta t^{Gen} = \sqrt{\left(\frac{2 \cdot m_1 \cdot \gamma_1 \cdot m_2 \gamma_2}{(m_1 \cdot \gamma_1 + m_2 \cdot \gamma_2)} \right) \cdot \frac{\left(E_1^{Gen} + E_2^{Gen}\right)}{\left(F^{Gen}\right)^2}} \quad (24)$$

Inspection of Equation 22 through Equation 24 reveals that in the absence of inter-vehicle friction, tire forces and rotation, each of these equations reduce to their parent forms developed in the original CRASH-type programs.

Missing Damage Dimensions

The *Generalized Force-Deflection Model* and the *Generalized Impact Work/Energy Model* in their present form (as derived in this paper) require knowledge of structural *A* and *B* stiffness coefficients and measured deformation profiles, Δc^R and Δw, for both vehicles. However, the Newton's third law expression for the impact using Equation 11 considers the total force acting equal and opposite between the vehicles during an oblique collision, resulting in the ability to predict the damage profile deformation depths of a vehicle if the structural stiffness values for both colliding vehicles and the damage profile of at least one vehicle in the impact are known. This results in Equation 25, hereto defined as the *Generalized Newtonian Deformation*

Prediction Model:

$$F_{known}^{Gen} = F_{unknown}^{Gen}$$

$$\Delta c_{unknown}^{Gen} = \frac{\frac{F_{known}^{Gen}}{\Delta w_{unknown}} - A_{unknown}}{B_{unknown}} \quad (25)$$

Where, F_{known}^{Gen} = generalized peak force calculated for the vehicle of known deformation

$F_{unknown}^{Gen}$ = generalized peak force for vehicle of unknown deformation by Newton's third law

$c_{unknown}^{Gen}$ = Newtonian predicted generalized deformation for vehicle of unknown deformation

$w_{unknown}$ = total deformation width for the vehicle of unknown deformation depth (quantity must be known or knowable)

$A_{unknown}$ and $B_{unknown}$ = structural stiffness values for vehicle of unknown deformation depth (these values must be known or knowable)

Equation 25 can be used in two different manners. First, if piece-wise measurements (individual sections measured for width and depth) of a damaged vehicle profile can be associated with distinct piece-wise segments of the vehicle with unknown deformation depth but known deformation width, the actual profile of the "unknown" vehicle can be predicted. This is useful for simulations where having a realistic damage profile prediction that can be compared to general diagrams or photographs is useful in solving the collision solution. Secondly, the weighted average deformation depth (average of depth as though distributed across the entire damage width) of the vehicle of unknown deformation depth can be determined over the known or knowable damage width, which will result in the same work done on the system, but will not produce a piecewise damage profile.

Missing Structural Stiffness Coefficients

The *Generalized Force-Deflection Model* provides the means by which the net generalized force of any generalized impact can be determined, and the measureable deformation profile to a vehicle with PDOF considerations provides the distance over which the net generalized force is applied. This basic concept is an expression of work/energy principles, in that the distance over which a force is applied to the system is equivalent to the total work done on the system.

$$\int F^{Gen} dx = E_{work}^{Gen}$$

Where, F^{Gen} is the generalized force magnitude applied at peak impulse, and dx is the differential distance over which the work on the system occurs

Consider a collision involving two vehicles where the damage profile of each vehicle has been measured or can be determined from photographic documentation. Unlike the application of the equations previously presented, this collision event has only one vehicle that has a known or knowable structural stiffness characteristic (A and B stiffness values), and the other associated vehicle or object does not have known or knowable structural stiffness values. If the weighted average damage for the vehicle of unknown structural stiffness is determinable, then by applying work/energy principles to a generalized vehicle-to-vehicle collision, a generalized expression for the work on the vehicle of unknown structural stiffness characteristics can be determined by Equation 26.

$$\sum_{j=0}^{n} F_j^{Gen} = \sum_{j=0}^{n} \left(A^{known} + B^{known} \cdot \Delta c_j^R \right) \cdot \frac{\Delta w_j}{\cos(\Pi^{known})}$$

$$\left(E_{work}^{Gen} \right)^{unknown} = \left(F^{Gen} \right)^{known} \cdot \left(\bar{C}^{unknown} \right) \cdot \left(1 + \tan^2(\Pi^{unknown}) \right) \quad (26)$$

Where, $\left(E_{work}^{Gen} \right)^{unknown}$ = Generalized work on vehicle with unknown structural stiffness values

$\left(F^{Gen} \right)^{known}$ = Generalized force applied to the vehicle of known A/B values

$\bar{C}^{unknown}$ = Weighted average deformation on vehicle of unknown A/B values

The weighted average deformation depth on the vehicle with unknown A/B stiffness values is calculated from the measured damage profile using Equation 27.

$$\overline{C}^{unknown} = \frac{\sum_{j=1}^{n} \Delta w_j \cdot \Delta c_j}{\sum_{j=1}^{n} \Delta w_j} \tag{27}$$

In fact, by applying Equation 26 in all cases, even when both structural stiffness values are known or knowable, the collision is forced to comply with Newton's third law, and a more accurate solution is produced, which will be demonstrated in the following section where these principles were applied to the RICSAC (Research Input for Computer Simulation of Automobile Collisions) staged collisions[16]. Equations 11, 17 through 20, and 22 through 27 make up the *Generalized Deformation and Total Velocity Change Analysis System of Equations*, or **G-DaTA** ΔV™.

Application of Methodology to RICSAC Staged Collisions

Equation 26 has no "vehicle type-specific" conditions or restrictions for its application of unknown structural stiffness values. In other words, the generalized form of Equation 26 has far-reaching and broader application beyond passenger vehicles, light trucks, vans, and SUVS, with the application to commercial vehicles, motorcycles, and even objects provided the damage profile and weighted average deformation can be determined.

By using Equation 26 for evaluating the generalized work done on any two-vehicle or vehicle-to-object collision system, the analysis of impacts with vehicles of unknown stiffness (due to the lack of testing, lack of model year overlap, or lack of adequate information regarding structural characteristics) is no longer a limiting factor. As long as one of the vehicle surfaces involved in an impact has known or knowable structural stiffness characteristics, any vehicle or object of unknown structural characteristics but known or knowable deformation profile can be analyzed using the deformation analysis methods presented. Additionally, as will be demonstrated through applying these principles to the 12 RICSAC tests, using these generalized models and only the stiffness coefficients for the frontal impacting vehicle (frontal A/B values only) and applying Equation 26 for the determination of work on the non-frontal impact vehicle (broadside or rear, or even by choosing one vehicle only in the head-on offset impacts) provides the best correlation of results.

The generalized models developed as summarized in this paper were tested against the 12 collisions as part of the RICSAC validation study that is used for the validation of computer models for collision analysis. The proper coordinate transformations of the accelerometer data as outlined in follow-on studies were also considered in order to ensure that the most accurate data for analysis was utilized[17]. **Figure 7 and Figure 8** shows the results and statistical analysis of the study using the generalized methods presented in this paper as compared to the RICSAC testing. Additionally, **Figure 9 and Figure 10** show the plots of the data fit, all of which fit within a ± 10% boundary using the generalized models.

The results of the testing show a high degree of correlation between the models developed and presented by this author to the RICSAC testing — much higher than has been achieved with any other known model to date. These results demonstrate that by carefully considering restitution, tire-ground forces, inter-vehicular friction, and rotational effects from off-set and/or oblique impacts, accurate and precise velocity change determinations for collisions can be made while considering only the structural stiffness characteristics of one vehicle.

RICSAC Test/Veh	ΔVx (kph)	ΔVx (mph)	ΔVy (kph)	ΔVy (mph)	PDOF (degrees)	RICSAC Test ΔVtotal (kph)	RICSAC Test ΔVtotal (mph)	RESULTS PIECEWISE DVtotal (mph)	Absolute Difference (mph)	Percent Difference (Calc-Test)	RESULTS AVERAGE DVtotal (mph)	Absolute Diff (mph)	Percent Difference (Calc-Test)	e rest.	h feet	ΔWscrape inches	% tire forces
1-V1	-18.2	-11.3	7.7	4.8	-22.9	19.8	12.3	12.3	0.1	0.6%	12.3	0.0	0.2%	0.05	1.0	35.9	75%
1-V2	25.7	16.0	-8.5	-5.3	-18.3	27.1	16.9	16.3	-0.6	-3.7%	16.2	-0.7	-4.0%		0.8		
2-V1	-27.8	-17.4	14.1	8.8	-26.8	31.2	19.5	19.9	0.4	2.1%	19.8	0.3	1.4%	0.00	1.1	41.7	75%
2-V2	-30.1	-18.8	-28.3	-17.7	43.3	41.3	25.8	26.0	0.2	0.6%	25.8	0.0	-0.2%		0.8		
3-V1	-15.3	-9.5	-1.1	-0.7	4.1	15.3	9.5	9.3	-0.3	-2.8%	10.5	0.9	8.9%	0.20	1.0	0	10%
3-V2	25.1	15.6	3.5	2.5	7.9	25.3	15.8	15.3	-0.5	-3.0%	17.3	1.5	8.7%		1.2		
4-V1	-30.1	-18.7	-0.5	-0.3	1.0	30.1	18.7	17.4	-1.3	-7.7%	19.1	0.4	2.2%	0.00	1.6	0	75%
4-V2	35.7	22.2	1.0	0.6	1.6	35.7	22.2	22.1	-0.1	-0.5%	24.3	2.1	8.7%		0.0		
5-V1	-26.1	-16.2	-0.2	-0.1	0.4	26.1	16.2	16.4	0.2	1.0%	16.2	0.0	-0.1%	0.05	2.4	0	75%
5-V2	41.0	25.5	2.4	1.5	3.4	41.1	25.5	25.4	-0.2	-0.8%	25.1	-0.4	-1.8%		1.4		
6-V1	-14.2	-8.8	3.9	2.4	-15.4	14.7	9.1	9.5	0.3	3.7%	9.3	0.2	2.2%	0.00	1.0	33.2	50%
6-V2	22.0	13.7	-6.8	-4.2	-17.2	23.0	14.3	14.2	-0.1	-0.6%	14.0	-0.3	-2.1%		1.1		
7-V1	-18.8	-11.7	4.0	2.5	-12.0	19.2	12.0	12.2	0.3	2.1%	12.9	1.0	7.5%	0.00	1.4	31.7	50%
7-V2	31.4	19.5	-5.6	-3.5	-10.1	31.9	19.8	18.3	-1.5	-8.5%	19.3	-0.5	-2.4%		2.1		
8-V1	-21.6	-13.4	10.6	6.6	-26.1	24.1	14.9	15.1	0.1	0.8%	15.2	0.3	1.8%	0.05	3.2	8.5	50%
8-V2	13.2	8.2	-11.9	-7.4	-42.0	17.8	11.0	11.4	0.3	2.9%	11.5	0.5	4.0%		2.6		
9-V1	-29.0	-18.0	13.7	8.5	-25.3	32.1	19.9	20.8	0.9	4.5%	20.9	1.0	4.8%	0.10	0.9	0	50%
9-V2	11.1	6.9	-7.1	-4.4	-32.6	13.2	8.2	8.3	0.1	1.1%	8.3	0.1	1.5%		0.9		
10-V1	-46.3	-28.8	29.1	18.1	-32.1	54.7	34.0	34.8	0.8	2.2%	34.4	0.4	1.2%	0.20	2.3	0	50%
10-V2	15.9	9.9	-12.4	-7.7	-37.9	20.2	12.5	12.4	-0.1	-1.2%	12.3	-0.3	-2.2%		2.0		
11-V1	-39.3	-24.4	2.6	1.6	-3.8	39.4	24.5	25.0	0.5	2.2%	24.8	0.4	1.5%	0.00	1.1	0	0%
11-V2	25.3	15.7	0.8	0.5	1.8	25.3	15.7	16.4	0.7	4.4%	16.3	0.6	3.8%		1.0		
12-V1	-65.7	-40.8	-1.3	-0.8	1.1	65.7	40.8	44.7	3.9	8.6%	43.8	3.0	6.9%	0.00	1.1	0	0%
12-V2	43.0	26.7	-2.4	-1.5	-3.2	43.1	26.7	29.7	2.9	9.9%	29.1	2.4	8.2%		1.1		

Figure 7

Summary of results for generalized model application to RICSAC testing.

Piecewise Matching Method			Weighted Average Method		
$\chi 2$ Test of fit	1.07	standard deviation of error	$\chi 2$ Test of fit	1.09	standard deviation of error
$\chi 2$ critical => (α=0.01)	10.2 (n=23)	±1.1 mph	$\chi 2$ critical => (α=0.01)	10.2 (n=23)	±0.9 mph
R^2 =>	0.989	±4.1%	R^2 =>	0.990	±3.9%
T-test => (α = 0.99)	0.24		T-test => (α = 0.99)	0.01	
critical=>	2.5		critical=>	2.5	
F-test => (α = 0.99)	0.69		F-test => (α = 0.99)	0.79	
critical=>	2.26		critical=>	2.26	

Figure 8
Statistical analysis of generalized models compared to RICSAC results.

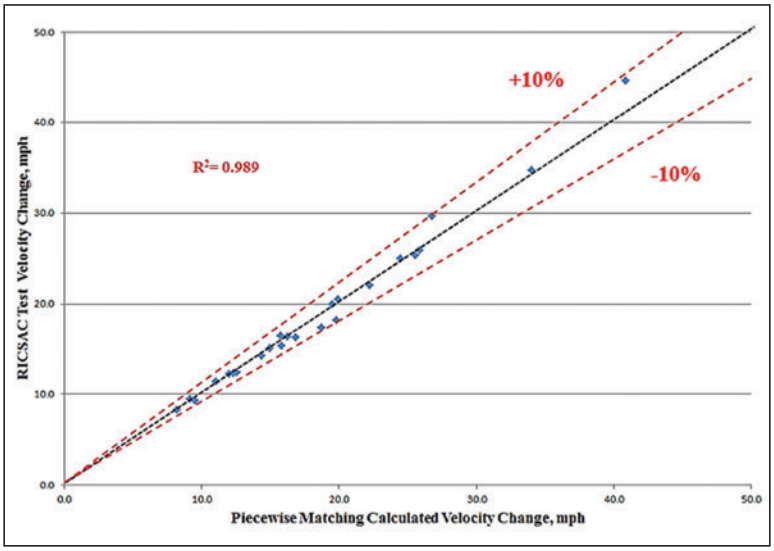

Figure 9
Results using Equation 26 for piecewise damage matching between vehicles.

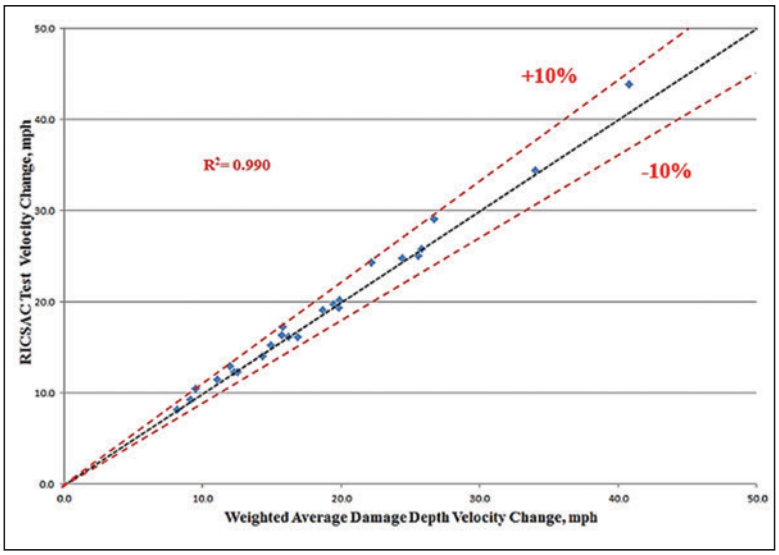

Figure 10
Results using Equation 26 for weighted average damage application.

G-DaTA ΔV™ Analysis Procedure

Application of the **G-DaTA ΔV™** system of equations starts with the documentation and measurement of vehicle deformation profiles for each vehicle into the form demonstrated in **Figure 1**. After tabulating the deformation profiles for the numerical analysis, the following general analytical steps provide the *Total Velocity Change* for two colliding vehicles:

1) Obtain vehicle weights, dimensions and determine inertial properties (Equation 10).

2) Determine the PDOF acting upon each vehicle (which will be directly opposite in direction when the vehicles are placed together at initial contact or maximum engagement; **Figure 6**).

3) Obtain vehicle A/B stiffness values for the selected vehicle in determining the *Generalized Force* acting equal and opposite between the colliding vehicles (Equation 11) based upon the following hierarchy:

   a) If both colliding vehicles have frontal stiffness values available, choose the A/B stiffness value for the vehicle with the greatest extent of measured damage (damage width and depth profile).

   b) Frontal A/B stiffness for vehicle with frontal impact damage for oblique side, broadside and rear-end impact configurations.

   c) A/B stiffness by vehicle struck surface (front, rear or side) if only one vehicle has an impact surface that is supported by test data regardless of impact configuration.

   d) If neither vehicle impact surface is supported, use a range of A/B stiffness factors for similar vehicles to establish a higher and lower bounding for the analysis.

4) Determine the work due to the non-conservative friction forces (Equations 17 and 18).

5) Determine the weighted average deformation depth for the vehicle which is not supported by A/B stiffness data or where A/B stiffness data was not used (Equation 27).

6) Determine the *Generalized Work* to produce compression of the vehicle structures in the form of permanent deformation (Equations 19 and 26).

7) Determine the time period to reach maximum impulse (Equation 24).

8) Determine the roadway friction (μ) and equivalent braking efficiency (n) for the vehicle whose tires act against the direction of impact force application (struck vehicle).

9) Determine an appropriate coefficient of restitution for the impact. The following are general rules for determining appropriate coefficients of restitution:

   e) Minor impacts with minor damage will have higher restitution values (see references 6 and 7).

   f) Even with extensive permanent damage profiles, ranging restitution between 0 and 0.1 may provide a greater confidence interval in the analysis results.

   g) When the impact involves an axle and/or wheel of a struck vehicle in an oblique side or broadside impact, restitution will range from 0.2 to 0.4 to account for the hardened zone of the axle and/or the "bounce" effect of impacting an inflated tire (see **Figure 7**).

10) Determine the *Total Velocity Change* for the vehicles produced by the impact event (Equations 22 and 23).

Outside of accurate deformation profile measurements, Step 3 is perhaps the most crucial step in the application of the **G-DaTA ΔV™** system of equations. The determination of the *Generalized Force* of the impact is completed for only one vehicle, not for both, since by Newton's third law the *Generalized Force* acting upon both vehicles is equal in magnitude but opposite in direction of application. If reliable stiffness data is available for both colliding vehicles and for the appropriate colliding surfaces (front, rear or side), then the determination of the *Total Velocity Change* for each vehicle can be calculated by applying the **G-DaTA ΔV™** system of equations twice and comparing results as a useful crosscheck or for providing a reasonable confidence interval for the analysis.

The following example of the application of the **G-DaTA ΔV™** system of equations is taken from RICSAC 6 staged collision involving the front of a 1974 Chevrolet Malibu (Vehicle 1, m_1) colliding with the right front side of a 1975 Volkswagen Rabbit (Vehicle 2, m_2) in an oblique off-set side impact. The impact velocity for both vehicles was recorded at 21.5 mph. The Chevrolet test weight was 4,310 pounds,

and the Volkswagen test weight was 2,640 pounds. Each vehicle contained two 49CFR Part 572 50th percentile anthropomorphic test devices (ATD). The ATDs in the Volkswagen were instrumented while the ATDs in the Chevrolet were un-instrumented during the collision. Data and results from this impact test are listed below.

Variables for the analysis were obtained from reported mass and deformation profiles, and data extrapolated from the collision diagram of **Figure 11** from the damage profiles matched at maximum engagement. As stiffness data was unavailable for the 1974 Chevrolet Malibu, the A and B structural stiffness data was obtained with permission from Neptune Engineering NEI Data Store for the similar 1970 Chevrolet Malibu four-door sedan. The **G-DaTA** ΔV™ system of equations were set up and analysis completed using PTC® MathCAD Prime 3.0.

The following are calculation results using the weighted average deformation depth analysis of Equation 27 applied to the VW Rabbit, the frontal stiffness A/B values for the Chevrolet Malibu for determining the *Generalized Force* using Equation 11 and the forced Newton's third law compliance for determining the *Generalized Work* of the vehicle without A/B stiffness values using Equation 26.

TEST RESULTS AND RECORDED VALUES:

$\Delta v1_{test} := -14.7\ kph = -9.134\ mph$ $\Delta tpeak := 0.095 \cdot sec$

$\Delta v2_{test} := 23.0 \cdot kph = 14.292\ mph$

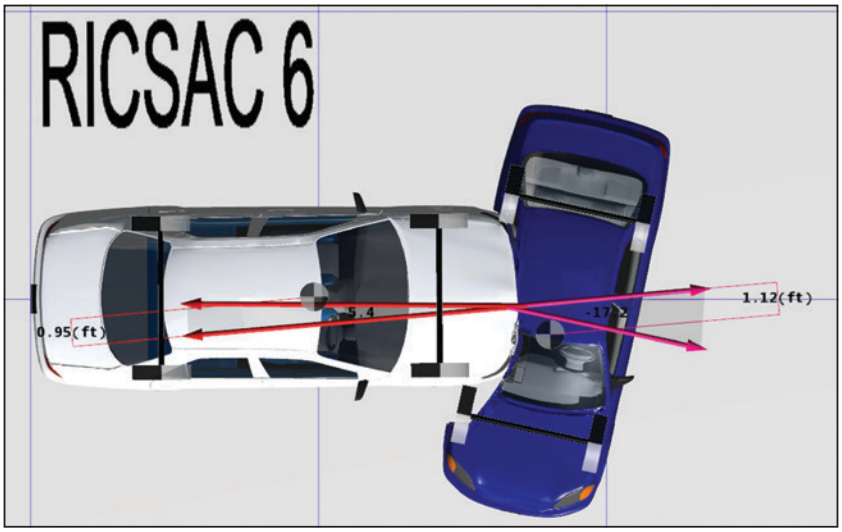

Figure 11
Maximum engagement PDOF diagram for RICSAC 6.

RICSAC 6: Measurements from scale damage sketches at same number of intervals

$$C1 := \begin{bmatrix} 0.0 \\ 0.5 \\ 0.5 \\ 1.25 \\ 1.5 \\ 1.75 \\ 2.25 \\ 0 \end{bmatrix} \cdot in \qquad W1 := \begin{bmatrix} 0.0 \\ 22.3 \\ 33.2 \\ 44.1 \\ 55.5 \\ 65.9 \\ 76.8 \\ 76.8 \end{bmatrix} \cdot in$$

$m_1 := \frac{4310 \cdot lb}{g} = 133.96 \ \frac{lb \cdot s^2}{ft}$ 1974 Chev. Malibu 4DR

$I1_{zz} := \frac{m_1}{13.8} \cdot \left((17.5 \cdot ft)^2 + (6.42 \cdot ft)^2 \right) \cdot (0.769) = (2.59 \cdot 10^3) \ lb \cdot ft \cdot s^2$

$A1 := 182 \cdot \frac{lb}{in}$ $B1 := 40 \cdot \frac{lb}{in^2}$ $h_1 := 1.0 \cdot ft$

$\Pi_{PDOF1} := -5.4 \cdot deg$ $\gamma_1 := \frac{I1_{zz}}{I1_{zz} + m_1 \cdot h_1^2}$

$$C2 := \begin{bmatrix} 0 \\ 4.0 \\ 12.0 \\ 17.9 \\ 21.5 \\ 17.0 \\ 8.25 \\ 0 \end{bmatrix} \cdot in \qquad W2 := \begin{bmatrix} 0 \\ 25.4 \\ 40.8 \\ 56.2 \\ 71.6 \\ 87.0 \\ 110.0 \\ 110.0 \end{bmatrix} \cdot in$$

$m_2 := \frac{2640 \cdot lb}{g} = 82.05 \ \frac{lb \cdot s^2}{ft}$ 1975 Volkswagen Rabbit 2DR

$I2_{zz} := \frac{m_2}{13.8} \cdot \left((14.25 \cdot ft)^2 + (5.75 \cdot ft)^2 \right) \cdot (0.769) = (1.08 \cdot 10^3) \ lb \cdot ft \cdot s^2$

$\Pi_{PDOF2} := (-17.2) \cdot deg$ $h_2 := 1.1 \cdot ft$

$e := 0.05$ $i := 0..6$ $\gamma_2 := \frac{I2_{zz}}{I2_{zz} + m_2 \cdot h_2^2}$

$C2\_bar := \frac{\sum_{i=1}^{6} \left(W2_{i+1} - W2_i \right) \cdot \left| \frac{C2_i + C2_{i+1}}{2} \right|}{W2_6} = 11.306 \ in$ weighted average deformation

$\Delta W_{scrape} := W2_6 - W1_6 = 33.2 \ in$ scraping distance on vehicle 2

$\mu_k := 0.5$ scraping friction coefficient

$\mu_r := 0.87$ surface friction coefficient

$n_2 := 50\%$ brake efficiency (broadside spin)

$$F1 := \sum_{i=0}^{6} \left(\left| A1 + B1 \cdot \left| \frac{C1_i + C1_{i+1}}{2} \right| \right| \right) \cdot \left(W1_{(i+1)} - W1_{(i)} \right) \cdot \left(\frac{1}{\cos(\Pi_{PDOF1})} \right) = (1.705 \cdot 10^4) \ lb$$

$$F_i := \left(\left| A1 + B1 \cdot \left| \frac{C1_i + C1_{i+1}}{2} \right| \right| \right) \cdot \left(W1_{i+1} - W1_i \right) \cdot \left(\frac{1}{\cos(\Pi_{PDOF1})} \right) \qquad F = \begin{bmatrix} 4.301 \cdot 10^3 \\ 2.212 \cdot 10^3 \\ 2.376 \cdot 10^3 \\ 2.714 \cdot 10^3 \\ 2.58 \cdot 10^3 \\ 2.869 \cdot 10^3 \\ 0 \end{bmatrix} lb$$

Weighted Average Deformation Depth Analysis:

$E2 := F1 \cdot C2\_bar \cdot \left(1 + \tan(\Pi_{PDOF2})^2 \right) = (1.76 \cdot 10^4) \ lb \cdot ft$

$E1_{Gen} := E1 + E1_{friction} = (6.031 \cdot 10^3) \ lb \cdot ft$

$E2_{Gen} := E2 + E2_{friction} = (1.987 \cdot 10^4) \ lb \cdot ft$

$\Delta tpeak := \sqrt{\left(\frac{2 \cdot m_1 \cdot \gamma_1 \cdot m_2 \cdot \gamma_2}{m_1 \cdot \gamma_1 + m_2 \cdot \gamma_2} \right) \cdot \frac{E1_{Gen} + E2_{Gen}}{F1^2}}$ $\Delta tpeak = 0.0918 \ s$

$\Delta V1 := -(1+e) \cdot \sqrt[2]{\left(\frac{2 \cdot m_2 \cdot \gamma_2 \cdot (E1_{Gen} + E2_{Gen})}{m_1 \cdot \gamma_1 \cdot (m_1 \cdot \gamma_1 + m_2 \cdot \gamma_2)} \right)} - \frac{m_2 \cdot (g \cdot \mu_r \cdot n_2) \cdot \Delta tpeak}{m_1} = -9.33 \ mph$

$\Delta V2 := (1+e) \cdot \sqrt[2]{\left(\frac{2 \cdot m_1 \cdot \gamma_1 \cdot (E1_{Gen} + E2_{Gen})}{m_2 \cdot \gamma_2 \cdot (m_1 \cdot \gamma_1 + m_2 \cdot \gamma_2)} \right)} - (g \cdot \mu_r \cdot n_2) \cdot \Delta tpeak = 14.031 \ mph$

$Diff1_{pw} := \Delta V1 - \Delta v1_{test} = -0.196 \ mph$ $Percent1_{pw} := \frac{\Delta V1 - \Delta v1_{test}}{\Delta V1} \cdot 100 = 2.1$

$Diff2_{pw} := \Delta V2 - \Delta v2_{test} = -0.261 \ mph$ $Percent2_{pw} := \frac{\Delta V2 - \Delta v2_{test}}{\Delta V2} \cdot 100 = -1.857$

Conclusions

The **G-DaTA** ΔV^{TM} system of equations presented consider restitution, tire-ground forces, inter-vehicular friction, and rotational effects that result during many collision events. In the absence of these factors, the equations revert back to their basic parent forms originally developed in the CRASH-based analysis models. Application to the RICSAC testing produced extremely good correlation and linear relationship between the known and calculated values between tests and within the entire testing as demonstrated by the F-test and chi-square test results, respectively, as well as the very linear correlation coefficients. The statistical analysis of the data indicates that any errors resulting between the calculated and test results are first of all minimal. Secondly, the difference between values is random in nature rather than any indication of systematic error. The application of the generalized models to the RICSAC testing is a first validation of the accuracy and precision of the presented methodologies.

The greatest use for the **G-DaTA** ΔV^{TM} system of equations is for the forensic analysis of real-world collision events; the methods should allow for greater confidence in the calculated total velocity change results when the analyst has adequate data to apply these principles. The presented methods have been applied by this author to the following impacts where vehicle and surface specific structural stiffness characteristics were either scarce or non-existent:

- Broadside or oblique side impacts.
- Rear end impacts.
- Impacts involving light trucks, vans, and sport utility vehicles where vehicle and surface specific structural stiffness values are scarce.
- Impacts involving heavy vehicles, buses, RVs, motorcycles, and other similar vehicles with few vehicle- and surface-specific data.
- Impacts with non-vehicular objects, or unique vehicles such as trailers or heavy equipment that deform when struck, but have no known structural stiffness data.

Additional future research should include the application of the **G-DaTA** ΔV^{TM} system of equations to vehicles and impact conditions outside of the RICSAC validation testing.

References

1. Campbell K. Energy basis for collision severity. SAE Technical Paper 740565. Warrendale PA: Society of Automotive Engineers; 1974.
2. CRASH III user's guide and technical manual. United States DOT, National Highway Traffic Safety Administration, National Center for Statistics and Analysis, Accident Investigation Division. Government Printing Office: Washington DC; 1986.
3. Tumbas N, Smith R. Measuring protocol for quantifying vehicle damage from an energy basis point of view. SAE Technical Paper 880072. Warrendale, PA: Society of Automotive Engineers; 1988.
4. Fricke L, Baker J. Traffic collision investigation. 10th Edition. Evanston, IL: Northwestern University Center for Public Safety; 2006. Chapter 3.
5. Rose N, Fenton S, Ziernicki R. An examination of the CRASH3 effective mass concept. SAE Technical Paper 2004-01-1181. Warrendale, PA: Society of Automotive Engineers International; 2004.
6. Ogden J. Forensic engineering analysis of damage and restitution in low velocity impacts. Journal of the National Academy of Forensic Engineers. 1999;16(2):11-34.
7. Ogden J. Methods of investigating and reconstructing minor damage low velocity motor vehicle accidents. Master of Science Thesis. University of Colorado Denver. October 1995.
8. Greenwood D. Advanced dynamics. New York: Cambridge University Press; 2003.
9. Hibbeler R. Engineering mechanics: statics and dynamics. 3rd ed. New York: Macmillan Publishing Company; 1983.
10. Nikravesh P. Planar multi-body dynamics: formulation, programming, and applications, Appendix A: Mass center and moment of inertia. Boca Raton: CRC Press (Taylor & Francis Group); 2008. 433-438.
11. Garrott W. Measured vehicle inertial parameters, NHTSA's data through September 1992. SAE Technical Paper 930897. Warrendale, PA: Society of Automotive Engineers; 1993.
12. Garrott W, Monk M, Christos W. Vehicle inertial parameters - measured values and approximations. SAE Technical Paper 881767. Warrendale, PA: Society of Automotive Engineers; 1988.
13. Neptune J. Overview of an HVE vehicle database. SAE Technical Paper 960896. Warrendale, PA: Society of Automotive Engineers; 1998.

14. Warner C, Smith G, James M, Germane G. Friction applications in accident reconstruction. SAE Technical Paper 830612. Warrendale, PA: Society of Automotive Engineers; 1983.
15. Marine M. On the concept of inter-vehicle friction and its application in automobile accident reconstruction. SAE Technical Paper 2007-01-0744. Warrendale, PA: Society of Automotive Engineers; 2007.
16. McHenry, Lynch, Segal. Research input for computer simulation of automobile collisions (Vol 1-4). U.S. DOT HS-7-01511. Washington, D.C.: National Highway Traffic Safety Administration; 1978.
17. McHenry B, McHenry R. RICSAC-97, a reevaluation of the reference set of full scale crash tests. SAE Technical Paper 970961. Warrendale, PA: Society of Automotive Engineers; 1997.